

ELECTRONIC SUPPORTING MATERIAL

Unusual magnetic damping effect in silver-cobalt ferrite nano-system

Surender K. Sharma,^{1, 2, 3} Jose Marcelo Vargas,⁴ Nicolás Manuel Vargas,⁵ Sebastian Castillo-Sepúlveda, Dora Altbir,⁵ Kleber Roberto Pirota,¹ Radek Zboril,³ Giorgio Zoppellaro,³ and Marcelo Knobel¹

¹Instituto de Física Gleb Wataghin, Universidade Estadual de Campinas (UNICAMP) Campinas, 13.083-859, SP, Brazil

²Laboratoire Interfaces Traitements Organisation et Dynamique des Systemes (ITODYS), UMR 7086 CNRS & Université Paris Diderot-Paris 7, Case 7090, 75205 Paris, Cedex 13, France

³Regional Centre of Advanced Technologies and Materials, Faculty of Science, Palacký University Olomouc, 771 46 Olomouc, Czech Republic

⁴Advanced Materials Research Institute, University of New Orleans, New Orleans, Louisiana 70148, USA

⁵Physics Department, Universidad de Santiago de Chile and CEDENNA, USACH, Santiago 917-0124, Chile

Corresponding authors:

[*surender76@gmail.com](mailto:surender76@gmail.com)

#knobel@ifi.unicamp.br

Experimental Section

The control and hetero nano-system of CoFe_2O_4 and $\text{CoFe}_2\text{O}_4\text{-Ag}$ were prepared by chemical route as published earlier¹⁻³ with some modifications as here reported.

Synthesis of magnetic CoFe_2O_4 nanoparticles

CoFe_2O_4 NPs with sizes in the range 2-13 nm were synthesized using thermal decomposition of $\text{Fe}(\text{acac})_3$ (2.0 mmol) and $\text{Co}(\text{acac})_3$ (1.0 mmol) in the presence of 1, 2-hexadecanediol (10 mmol) and the surfactants oleic acid (6 mmol) and oleylamine (6 mmol) in 20 mL of phenylether. This mixture was gently heated at 200°C for 60 minutes under continuous Ar flux with intermediate stirring. The above mixture was slowly heated up to a final temperature of 265°C for 120 minutes under Ar flux with heating rate of ~ 6 °C/min. Finally, the solution was cooled down to room temperature. The NPs were washed adding excess of ethanol and centrifugation was carried out at 3800 rpm for 10 minutes. This procedure was repeated 3-4 times by dispersing the NPs in toluene, adding excess of ethanol followed by centrifugation. Finally, the NPs were dispersed in toluene (concentration of 0.05 g/ml) for the long-term storage. The sample has been thereafter designated as CFO1. In order to make the larger nanoparticles, CFO1 nanoparticles were dissolved in toluene (5 mL) with concentrations of 7 mg/mL together with same amounts of $\text{Fe}(\text{acac})_3$, 1,2 hexadecanediol, oleic acid, oleylamine and phenylether as described above. The particles of approximate size of 10-11 nm were found using the same washing and isolation procedure as used for CFO1 sample. The sample is thereafter labeled as CFO in the main article. This is used as seeds to grow CFO-Ag hetero nano-system.

Synthesis of $\text{CoFe}_2\text{O}_4\text{-Ag}$ hetero nano-system

To prepare the $\text{CoFe}_2\text{O}_4\text{-Ag}$ hetero nano-system, 10-11 nm CoFe_2O_4 nanoparticles (CFO) were dissolved in 5 mL toluene with concentration of 5 mg/mL. Firstly, the Ag metallic precursor ($\text{C}_{54}\text{H}_{45}\text{NO}_3\text{P}_3\text{Ag}$) was prepared from the stoichiometric amount of silver nitrate (1.1 mmol) and triphenylphosphine (3 mmol), mixed in 10 mL of warm acetonitrile as described in our earlier publication [1]. A white powder was obtained after heating at 80 °C in an inert atmosphere for 3 hours. Thereafter, 2 mmol of oleylamine and 2 mmol of oleic acid were slowly added to the phenylether (20 mL) and CoFe_2O_4 seeds (CFO, 25 mg) where the Ag metallic precursor has been placed (5 mg Ag, corresponding to 44.4 mg of metallic precursor). This mixture was first heated at 100°C for 30 minutes, then 200°C for 60 minutes and finally kept at 265°C for 120 minutes under Ar atmosphere and then cooled to room temperature. The NPs were isolated using the same procedure described above. The obtained particles can be easily dispersed in non-polar solvents. The sample was labelled as CFO-Ag. Note all these particles are coated by organic molecules of oleic acid that avoid the direct contact between particles.

Apparatus

The particle diameter and distribution was screened by transmission electron microscopy (TEM) as well as small angle x-ray scattering (SAXS). For SAXS measurements, the sample was prepared in colloidal solution of toluene at 1:20 volume concentration. The structure was determined by X-ray diffraction (XRD) (Philips, X-PERT) with Cu K_{α} radiations. The dc/ac magnetic properties were measured on dried powdered samples using both Quantum Design SQUID and PPMS magnetometers, respectively. The dc magnetic properties were measured with fields up to 70 kOe and temperatures from 50-350 K. The ZFC and FC measurements were carried out as follow: the sample was first cooled down from 350 K to 50 K in a zero magnetic field, then a static magnetic field ($H = 50$ Oe) was applied and M_{ZFC} was measured during warming up from 50 K to 350 K; finally the sample was cooled down to 50 K under the same field and M_{FC} was measured during the cooling cycle. The field dependence of isothermal remanent magnetization (IRM) and DCD (direct current demagnetization) remanent magnetizations were measured at a temperature of 50 K as follows: the initial state for an IRM measurement is the totally demagnetized ZFC sample. A field was applied for 10 s, then it was switched off and the remanent magnetization was measured, (M_{IRM}). The process was repeated, increasing the field up to 50 kOe. In case of DCD measurements, a field of -50 kOe was applied for 10 s; then a small external field in the direction opposite to that of magnetization was applied and, after 10 s, it was switched off and the remanent magnetization (M_{DCD}) was measured. This was repeated, increasing the field up to 50 kOe⁴. The real and imaginary parts of the ac magnetic susceptibility were measured at frequencies between $10 \text{ Hz} \leq f \leq 10 \text{ kHz}$ in external ac field amplitude of 5 Oe on a commercial Physical Property Measurement System (PPMS) in the temperature range 50-350 K. Mössbauer spectrum was measured employing a home-made Mössbauer spectrometer working in a constant acceleration mode and equipped with a ⁵⁷Co (Rh) source with an activity of 50 mCi. The sample was placed inside the chamber of a closed-helium-cycle cryostat enabling to set the temperature in the range from 15 to 295 K. The isomer shift values were referred to α -Fe foil at room temperature.

Micromagnetics simulation details

Micromagnetics simulations (MMS) were performed using Oriented Micro Magnetic Framework software (OOMMF)⁵ in static and oscillating magnetic fields, where the magnetization dynamics is governed by the Landau–Lifshitz–Gilbert (LLG) equation⁶. Thus, the ferromagnetic system is spatially divided into cubic cells within each one the magnetization is assumed to be uniform. In the MMS framework, the properties of any material can be obtained from the stiffness constant, \mathbf{A} and the saturation magnetization, \mathbf{M}_s . The CFO nanoparticles were modeled here as a single homogeneous nanoparticle with a diameter of ~ 10 nm, using $\mathbf{A} \sim 30 \times 10^{-12}$ A/m, $\mathbf{M}_s \sim 1400 \times 10^3$ J/m, and uniaxial anisotropy of $\mathbf{K} \sim 900 \times 10^3$ J/m³. These values account for the increase of ferrite parameters, \mathbf{A} , \mathbf{K} and

M_s , due to some Co aggregation. In the first approximation, the CFO-Ag sample was modeled as a pseudo core-shell system made by those CFO nanoparticles that are more tightly interacting with Ag and the remaining CFO nanoparticles that are weakly interacting with Ag. Although this is a simplistic consideration which can be supported on the fact of the double distribution obtained through the analysis of the χ_{IRR} as well as HRTEM imaging. Actually, the effect of Ag attached to the CFO is much more complex than this, with electronic hybridization effects. For the core we have used the same parameters mentioned above with a diameter of ~ 9 nm. This is in fact the size of CFO nanoparticles themselves but considered here as only those in close contacts with Ag nanoparticles. For the shell, with a 3 nm thickness, we assume slightly lower values for $A \sim 9 \times 10^{-12}$ A/m, $M_s \sim 200 \times 10^3$ J/m, and $K \sim 5.7 \times 10^2$ J/m³ based on the fact of Ag aggregation which in turn decrease the magnetic character of the shell formed by the CFO nanoparticles that are weakly interacting. In all the cases the damping parameter was chosen as 0.5 for static simulations. It is worth mentioning that, in these simulations, the interparticle interactions were neglected.

Additional experimental data

- Rietveld refinement of Powder X-ray diffraction patterns (XRD)

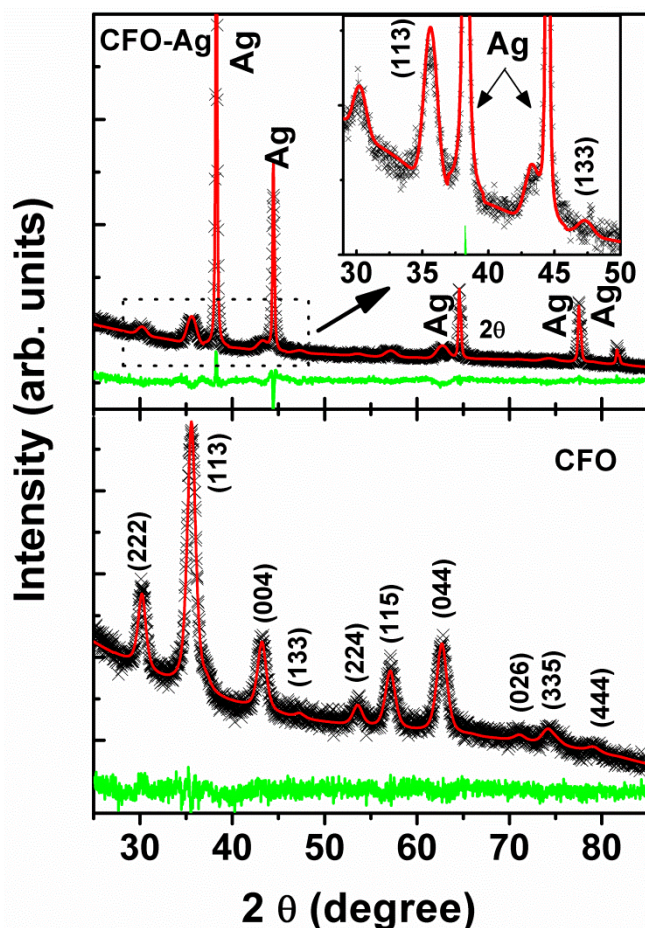


FIGURE S1. Rietveld refinement of X-ray diffraction (XRD) patterns for CFO and CFO-Ag hetero nano-system prepared using seeds of CoFe_2O_4 .

Figure S1 shows the x-ray diffraction (XRD) patterns for the two investigated samples, CFO and CFO-Ag, analyzed using a full profile fitting program based on the Rietveld method. The detailed analysis of the peak positions and their relative intensities confirm the presence of the single cubic phase of CoFe_2O_4 with space group $\text{Fm}\bar{3}\text{m}$ (JCPDS No. 22- 1086) and a lattice parameter $a = 8.398(2)$ Å. The resulting average crystalline particle diameter is $D_{\text{XRD}} = 12 \pm 1.0$ nm. Contrary, CFO-Ag one can clearly see that the pattern consist of strong contribution of the sharp peaks indexed as Ag NPs encompassed by the very broad peaks indexed as CoFe_2O_4 spinel ferrite. We have observed no shifting in the peak positions

for CoFe_2O_4 and/or Ag, compared to reference/standard bulk sample thereby indicating that the lattice structure remains intact for the CFO-Ag NPs.

- **Small Angle X-ray scattering data (SAX)**

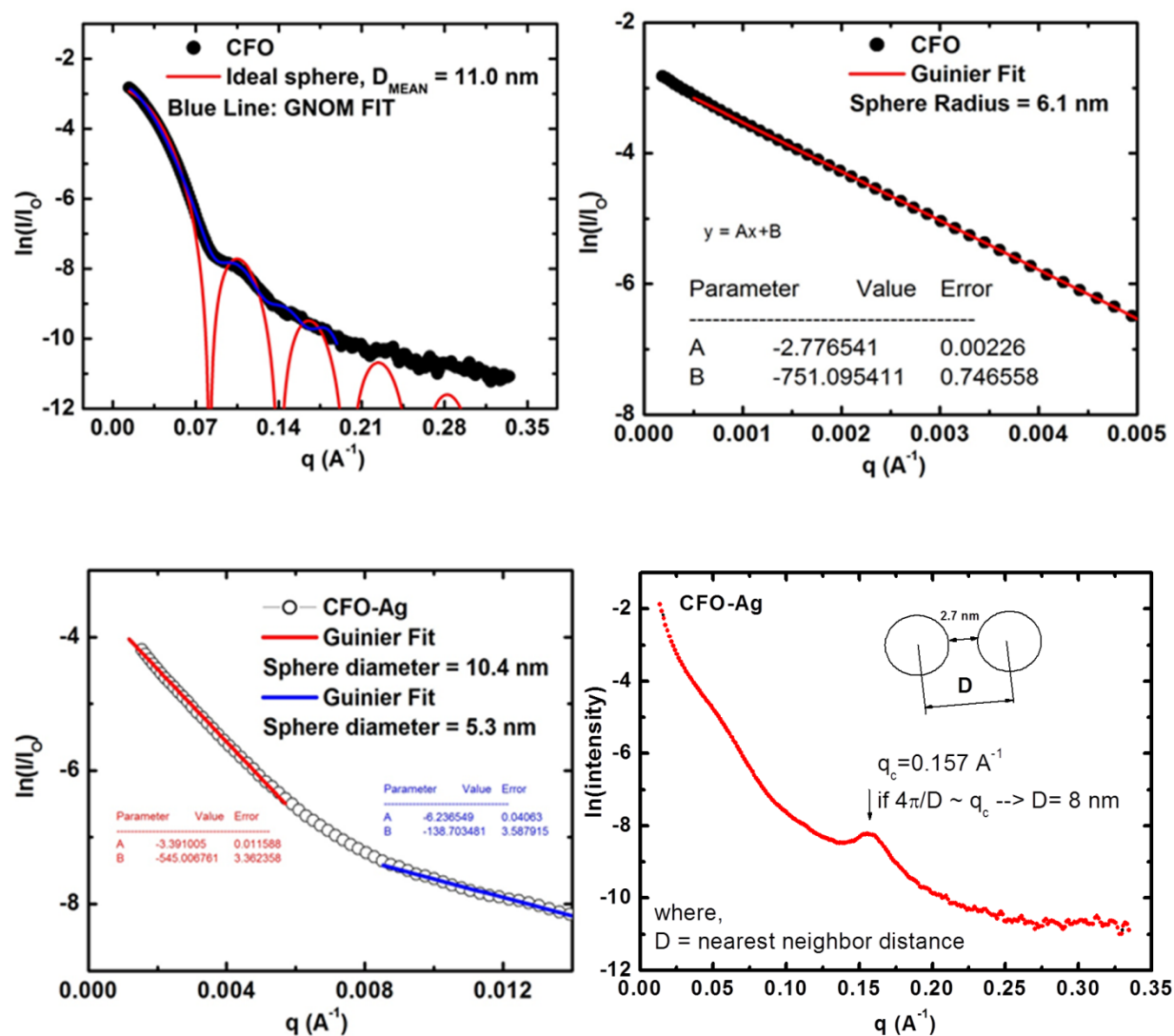


FIGURE S2. The Small angle x-ray scattering (SAXS) data for CFO (upper panels) and CFO-Ag (lower panels) together with Guinier's fittings.

Figure S2 shows the SAXS data for the control CFO sample and the Guinier's fitting for both CFO and CFO-Ag samples. We have observed two different slopes in the Guinier's plot for the CFO-Ag sample as compared to one in CFO: a linear fit below $q = 0.005 \text{ \AA}^{-1}$ which correspond to the CoFe_2O_4

nanoparticles, whereas the second one lies between 0.009-0.013 Å⁻¹ for the Ag nanoparticles. Further, a broad peak is observed around 0.15 Å⁻¹ validating the agglomeration effect for CFO-Ag sample.

- **Mössbauer Spectroscopy**

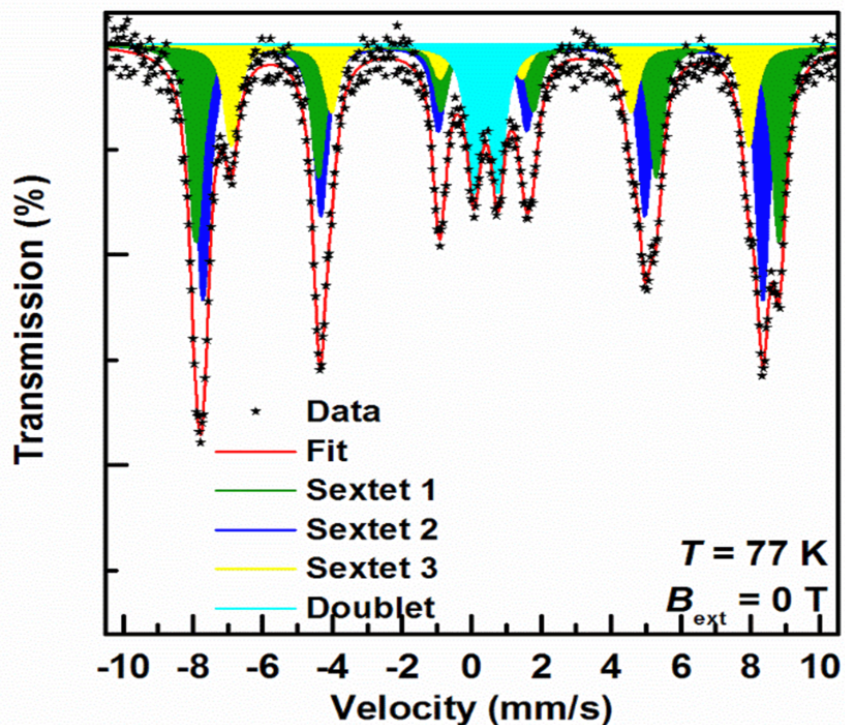


Figure S3. Zero-field Mössbauer spectrum of the CFO-Ag sample measured at a temperature of 77 K.

The interactions (direct/indirect) arising from contacts between Ag and CoFe₂O₄ in CFO-Ag became evident from analysis of the zero field Mössbauer spectrum ($T= 77$ K) that showed appearance of four spectral components, i.e., three sextets and one doublet. The two sextets (coded sextet 1-green and sextet 2-blue in Fig S3) encompassed high values of the magnetic hyperfine field ($B_{\text{hf}} = 52.0 \pm 0.3$ T and 49.9 ± 0.3 T) that reflected the typical spinel crystal structure of CFO⁷, whereas the third sextet (sextet 3- yellow) with lowest value of magnetic hyperfine field ($B_{\text{hf}} = 46.2 \pm 0.3$ T) originated from the Fe cations located in the surface layers. The presence of non-zero quadrupole splitting value suggested changes in the electron charge distribution, effect that could be induced from the distorted local surrounding of the surface atoms or by interaction mechanism from non-magnetic Ag close to the CoFe₂O₄ surface. Compared to conventional and isolated CoFe₂O₄ nanoparticles of similar dimension and/or size distribution⁸, the significant increase of the quadrupole splitting observed here cannot be solely driven by the rise in the value of the surface-to-volume ratio.

Table S1. Values of the Mössbauer hyperfine parameters, derived from the zero-field Mössbauer spectrum recorded at a temperature of 77 K, where δ is the isomer shift, ΔE_Q is the quadrupole splitting, B_{hf} is the hyperfine magnetic field, and RA is the relative spectral area of individual spectral components.

Component	$\delta \pm 0.01$	$\Delta E_Q \pm 0.01$	$B_{\text{hf}} \pm 0.3$	$RA \pm 1$	Assignment
	(mm/s)	(mm/s)	(T)	(%)	
Sextet 1	0.47	0.01	52.0	32	Octahedral cation sites
Sextet 2	0.32	0.01	49.9	41	Tetrahedral cation sites
Sextet 3	0.40	0.26	46.2	16	Surface cation sites under interaction
Doublet	0.41	0.69	-----	11	Superparamagnetic component

- dc Magnetization Measurements

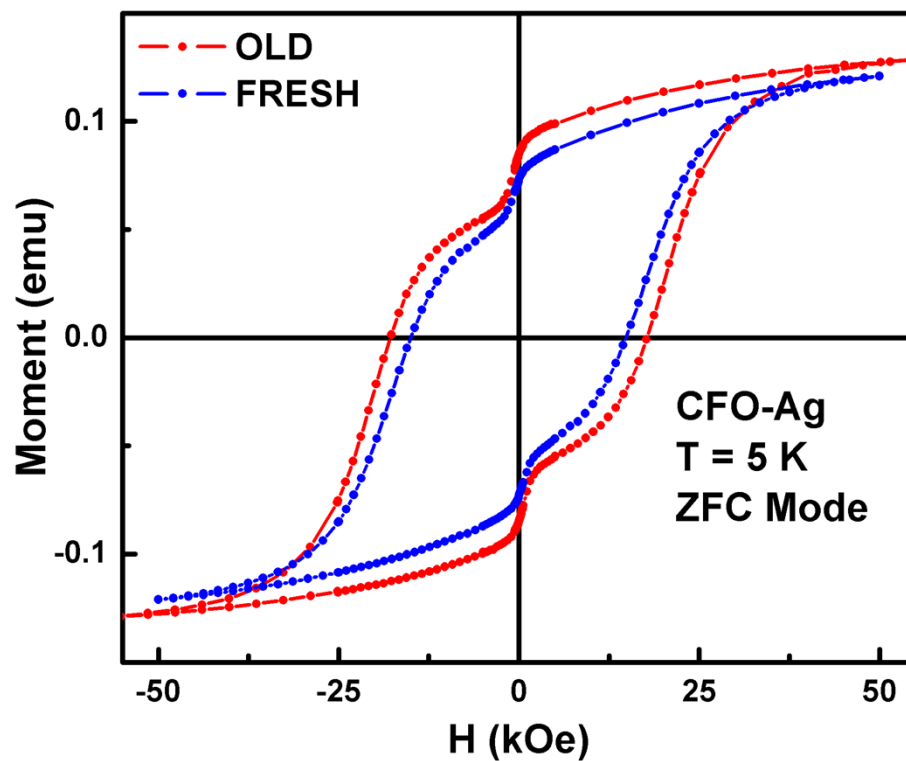


Figure S4 .Hysteresis curves for CFO-Ag hetero nano-system measured at 5 K in zero-field-cooled (ZFC) mode from above room temperature (red circle-old) and the same sample measured after six months (blue circle-fresh), showing no appreciable change in the coercivity of the sample. Note: The measurements have been done on two different Quantum design SQUID magnetometers as well as different applied magnetic fields (± 70 kOe or ± 50 kOe).

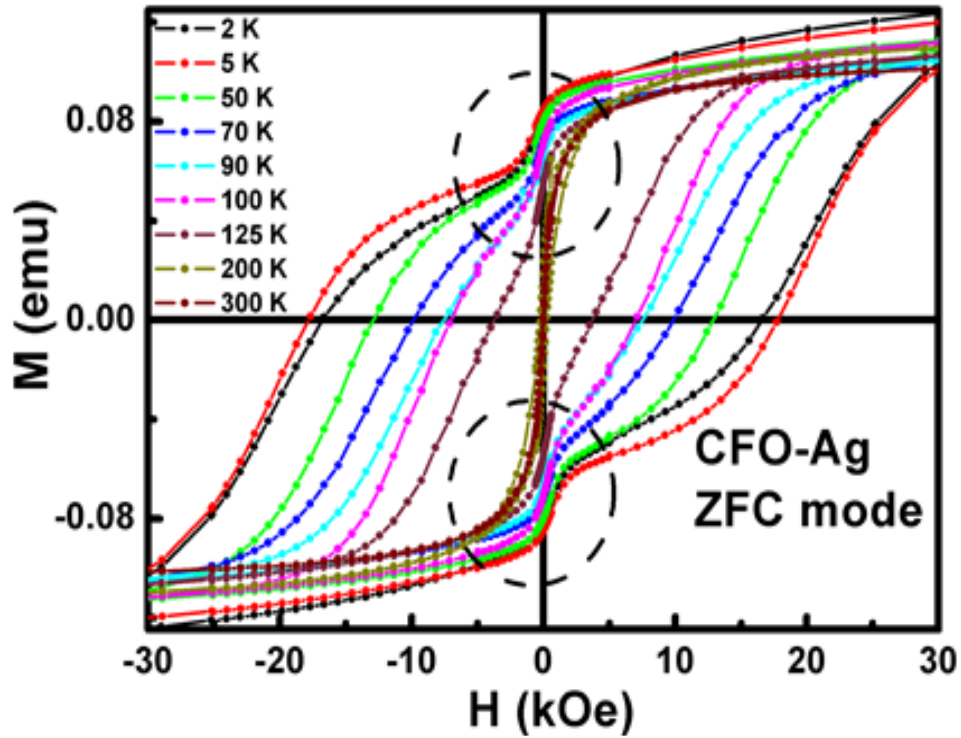


Figure S5 .Temperature dependent Hysteresis curves for CFO-Ag hetero nano-system measured in zero-field-cooled (ZFC) mode showing how the damping effect observed close to zero magnetic fields are diminishing upon approaching the sample temperature toward the blocking temperature of the CFO-Ag system.

- Arrhenius and Vogel-Fulcher plots from ac susceptibility measurements

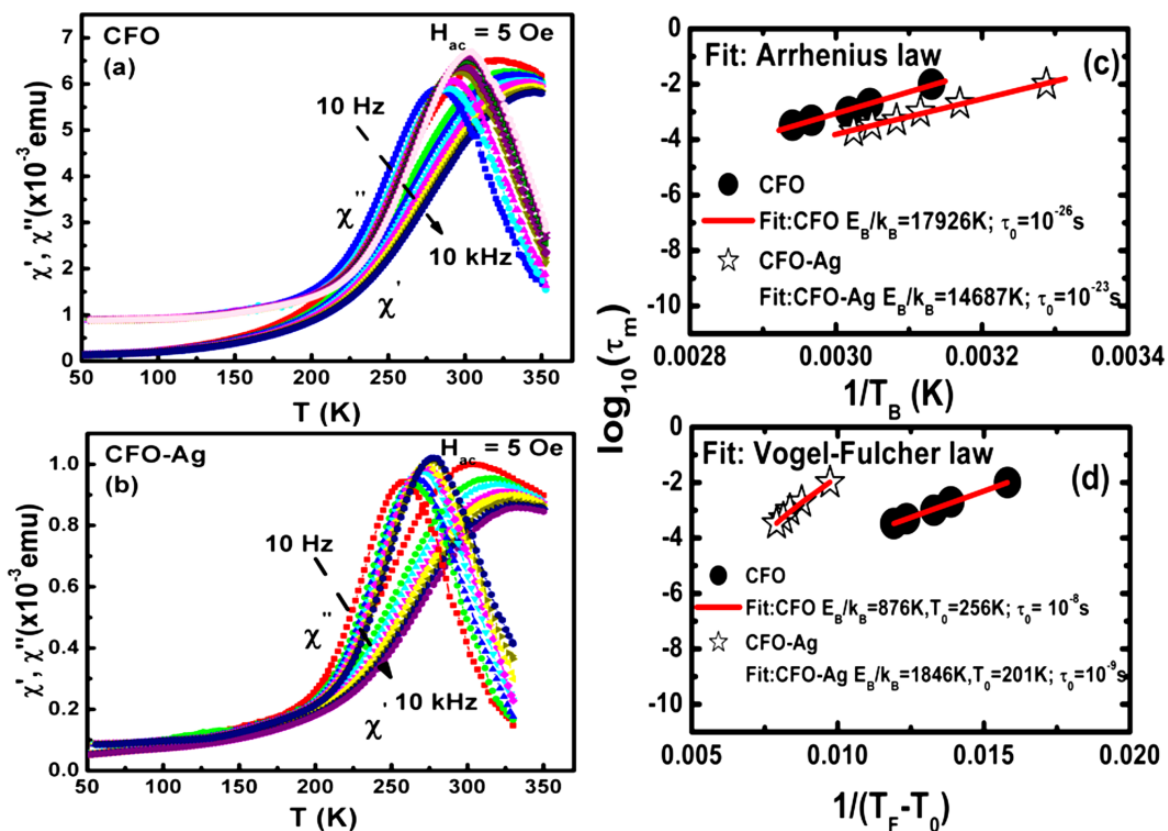


FIGURE S6. Panel (a) and (b) show the T -dependence of the real part of the ac susceptibility. Panel (c) & (d) show the variation of T_B in the classical Arrhenius and Vogel-Fulcher plot of $\log_{10}(\tau)$ vs. $1/T$.

REFERENCES

- ¹ G. Lopes et al., *Journal of Physical Chemistry C*, **114 (22)**, 10148 (2010).
- ² J. M. Vargas et al., *Journal of Applied Physics*, **109 (7)**, 07B536 (2011).
- ³ S. K. Sharma et al., *Journal of Applied Physics*, **109 (7)**, 07B530 (2011).
- ⁴ D. Peddis, C. Cannas, G. Piccaluga, E. Agostinelli, and D Fiorani, *Nanotech.* **21**, 125705 (2010).
- ⁵ M. Donahue, and D. G. Porter, *OOMMF User's Guide, Version 1.0*, Interagency Report NISTIR 6376 (National Institute of Standard and Technology, Gaithersburg, MD, 1999); <http://math.nist.gov/oommf>
- ⁶ L. D. Landau and E. Lifshitz, *Phys. Z. Sowjetunion* **8**, 153 (1935) ; T. L. Gilbert, *Phys. Rev.* **100**, 1243 (1955)
- ⁷ A. T. Ngo, P. Bonville, and M. P. Pileni, *J. Appl. Phys.* **89**, 3370 (2001).
- ⁸ G. C. Papaefthymiou, E. Devlin, A. Simopoulos, D. K. Yi, S. N. Riduan, S. S. Lee, J. Y. Ying, *Phys. Rev. B* **80**, 024406 (2009); D. C. Gregor, M. Hermanek, D. Jancik, J. Pechousek, J. Filip, J. Hrbac, R. Zboril, *Eur. J. Inorg. Chem.* **16**, 2343 (2010).